Saudi Journal of Biological Sciences 29 (2022) 3354–3365

Contents lists available at ScienceDirect

Saudi Journal of Biological Sciences

journal homepage: www.sciencedirect.com

Original article

Anticancer effect of selenium/chitosan/polyethylene glycol/allyl isothiocyanate nanocomposites against diethylnitrosamine-induced liver cancer in rats

Cheng Li [a], Saleh H. Salmen [b], Tahani Awad Alahmadi [c], Vishnu Priya Veeraraghavan [d], Krishna Mohan Surapaneni [e], Nandakumar Natarajan [f], Senthilkumar Subramanian [g,*]

[a] Department of Interventional Medicine, The First Affiliated Hospital of Wenzhou Medical University, South Bai Xiang Street, Ouhai District, Wenzhou, Zhejiang 325000, China
[b] Department of Botany and Microbiology, College of Science, King Saud University, PO Box-2455, Riyadh 11451, Saudi Arabia
[c] Department of Pediatrics, College of Medicine and King Khalid University Hospital, King Saud University, Medical City, PO Box-2925, Riyadh 11461, Saudi Arabia
[d] Centre of Molecular Medicine and Diagnostics (COMManD), Department of Biochemistry, Saveetha Dental College, Saveetha Institute of Medical and Technical Sciences, Saveetha University, Chennai 600 077, India.
[e] Department of Biochemistry, Panimalar Medical College Hospital & Research Institute, Varadharajapuram, Poonamallee, Chennai 600 123, India.
[f] Department of Surgery, Immunogenetics and Transplantation Laboratory, University of California San Francisco, San Francisco, CA, USA
[g] School of Medicine, College of Medicine and Health Science, Jigjiga University, Jigjiga, Ethiopia

ARTICLE INFO

Article history:
Received 19 January 2022
Revised 8 February 2022
Accepted 9 February 2022
Available online 11 February 2022

Keywords:
8-Hydroxy-2′-deoxyguanosine
Nano-drug delivery
Liver cancer
Allyl isothiocyanate
Diethylnitrosamine

ABSTRACT

Background: Nano-based drug delivery systems have shown several advantages in cancer treatment like specific targeting of cancer cells, good pharmacokinetics, and lesser adverse effects. Liver cancer is a fifth most common cancer and third leading cause of cancer-related mortalities worldwide.
Objective: The present study focusses to formulate the selenium (S)/chitosan (C)/polyethylene glycol (Pg)/allyl isothiocyanate (AI) nanocomposites (SCPg-AI-NCs) and assess its therapeutic properties against the diethylnitrosamine (DEN)-induced liver cancer in rats via inhibition of oxidative stress and tumor markers.
Methodology: The SCPg-AI-NCs were synthesized by ionic gelation technique and characterized by various characterization techniques. The liver cancer was induced to the rats by injecting a DEN (200 mg/kg) on the 8th day of experiment. Then DEN-induced rats treated with 10 mg/kg of formulated SCPg-AI-NCs an hour before DEN administration for 16 weeks. The 8-hydroxy-2′ -deoxyguanosine (8-OHdG) content, albumin, globulin, and total protein were examined by standard methods. The level of glutathione (GSH), vitamin-C & -E, and superoxide dismutase (SOD), catalase (CAT), glutathione peroxidase (GPx), and glutathione reductase (GR) activities were examined using assay kits. The liver marker enzymes i.e., alanine transaminase (ALT), aspartate tansaminase (AST), γ-glutamyl transaminase (GGT), lactate dehydrogenase (LDH), and alkaline phosphatase (ALP) activities, alpha fetoprotein (AFP) and carcinoembryonic antigen (CEA), Bax, and Bcl-2 levels, and caspase-3&9 activities was examined using assay kits and the liver histopathology was assessed microscopically by hematoxylin and eosin staining method. The effect of formulated SCPg-AI-NCs on the viability and apoptotic cell death on the HepG2 cells were examined using MTT and dual staining assays, respectively.
Results: The results of different characterization studies demonstrated the formation of SCPg-AI-NCs with tetragonal shape, narrowed distribution, and size ranging from 390 to 450 nm. The formulated SCPg-AI-NCs treated liver cancer rats indicated the reduced levels of 8-OHdG, albumin, globulin, and total protein. The SCPg-AI-NCs treatment appreciably improved the GSH, vitamin-C & -E contents, and SOD, CAT, GPx, and GR activities in the serum of liver cancer rats. The SCPg-AI-NCs treatment remarkably reduced the liver marker enzyme activities in the DEN-induced rats. The SCPg-AI-NCs treatment decreased the AFP

* Corresponding author.
E-mail address: ksslkumar@gmail.com (S. Subramanian).
Peer review under responsibility of King Saud University.

Production and hosting by Elsevier

https://doi.org/10.1016/j.sjbs.2022.02.012

and CEA contents and enhanced the Bax and caspase 3&9 activities in the DEN-induced rats. The SCPg-AI-NCs effectively decreased the cell viability and induced apoptosis in the HepG2 cells.
Conclusion: The present findings suggested that the formulated SCPg-AI-NCs remarkably inhibited the DEN-induced liver carcinogenesis in rats. These findings provide an evidence that SCPg-AI-NCs can be a promising anticancer nano-drug in the future to treat the liver carcinogenesis.

1. Introduction

The nanoscale drug designing and nano-based drug delivery systems have shown several advantages in cancer treatment because of its unique properties such as solubility, bioavailability, and drug release profiles. This, can subsequently lead to the development and advancement of suitable route of administration, lesser adverse effects, reduced toxicity, increased bio-diffusivity, and increased drug-life period (Palazzolo et al., 2018). The bio-engineered drug delivery systems are either targeted to the specific site or intended to controlled drug release at a specific location (Lu et al., 2016; Barahuie et al., 2013). In recent times, there has been tremendous advancements in the field of targeted drug delivery systems to deliver drugs to its targeted sites to treat the several diseases (Mintz and Leblanc, 2021).

Nano-oncology is an application of nano-biotechnology in the treatment of cancers (Sun et al., 2018; Wu et al., 2018). Especially, it can decrease the adverse effects induced by chemotherapeutic drugs, increase the life expectancy and quality of patients (Meng et al., 2019). Numerous previous literatures highlighted that nano-materials can penetrate into cells, tissues, and organs, releasing drugs at specific spots that are highly challenging to reach with traditional chemotherapeutic drugs (Yang et al., 2020; Wu et al., 2020). Recently, nano-drug formulations have frequently been studied in amalgamation with natural products to minimize the toxicity. Consequently, consuming green nano-formulations for drug delivery systems can increase the therapeutic property and minimize the adverse effects of the drugs (Milewska et al., 2021; Tan et al., 2014).

The nanocarriers are considered as an effective vehicles to deliver a drugs at specific location. The nanocarriers has the potential to decrease the cytotoxicity and improve the therapeutic effects of chemotherapeutic drugs (Zhang et al., 2018). The majority of the chemotherapy drugs have high cytotoxicity, low molecular weight, and less specificity with increased adverse effects (Lata et al., 2017). Selenium is a natural essential micronutrient, which has received substantial research interest in the fields of biology and medicine due to its specific pharmacological properties, particularly cancer prevention and improvement of immunity (Skalickova et al., 2017; Tan et al., 2018). It has been reported that the many cancer patients are selenium deficient (Zhang et al., 2016). Chitosan is a natural polysaccharide and has unique properties, which makes it ideal for several targeted drug delivery systems (Shaban et al., 2020; Li et al., 2018).

Allyl isothiocyanate is a natural bioactive compound found largely in the plants from Cruciferae family and are highlighted to show several pharmacological effects such as neuroprotective (Subedi et al., 2017), anticancer (Bhattacharya et al., 2010), antidiabetic (Sahin et al., 2019), antifungal (Olivier et al., 1999), and anti-ulcerative colitis (Kim et al., 2018) activities. Many previous literatures highlighted that the allyl isothiocyanate effectively inhibited the proliferation and triggered apoptosis in numerous tumor cells, such as breast, bladder (Savio et al., 2015), lung (Tripathi et al., 2015), colon (Lai et al., 2014), liver (Hwang and Kim, 2009), prostate (Xu et al., 2006), cervical (Qin et al., 2018), and oral (Chang et al., 2021) cancer cells.

Liver cancer is a fifth most common cancer and third leading cause of cancer-associated deaths worldwide with above 800,000 mortalities each year (Ikeda, 2019; Bray et al., 2018). The normal survival period of liver cancer patients without treatment is reported to be a 1–3 months. Presently, the surgical resection, chemo and radiotherapies are the most hopeful strategies for the treatment of liver cancer. Though, only 15% of patients are reported to be eligible for the surgical treatments. The remaining 85% of patients were turn to other therapies due to their poor prognosis, metastasis, and improper liver function (e.g., underlying cirrhosis) (Liccioni et al., 2014). In order to overcome these issues, the effective therapeutic strategies are highly demanded in recent times with increased therapeutic potentials. Hence, the present research focusses to formulate the selenium/chitosan/polyethylene glycol/allyl isothiocyanate nanocomposites (SCPg-AI-NCs) and examine its therapeutic properties against the DEN-induced liver cancer in rats via inhibition of oxidative stress and tumor markers.

2. Materials and methods

2.1. Chemicals

Allyl isothiocyanate, selenium, chitosan, polyethylene glycol, and additional chemicals and reagents were procured from Sigma-Aldrich, USA. The marker specific assay kits were acquired from Thermofisher Scientific and Biocompare, USA.

2.2. Synthesis of SCPg-AI-NCs

The ionic gelation technique was adopted to formulate the NCs, which comprises selenium, chitosan, polyethylene glycol, and allyl isothiocyanate. In brief manner, 20 mg of allyl isothiocyanate was prepared in 20 ml of water and added to the 200 ml of chitosan solution (1% wt/volume in aqueous acetic acid) under the continuous stirring until the development of suspension system. After that, this suspension was ultrasonicated for the reduction of nano particle droplets in the suspension. Then, the suspension containing chitosan and allyl isothiocyanate was added in drop-wise manner into the enteric polymer solution for the purpose of coating of developed particles. Here, the polyethylene glycol polymer suspension was used for the coating purpose.

The micro-volume flow titration technique was performed for the coating process and after that the developed nanoparticles powder was taken by desiccating the final solution using spray pyrolysis at 80–100 °C and 5 L/min airflow (Wathoni et al., 2019).

2.3. Characterization of formulated SCPg-AI-NCs

The UV–visible spectral study was performed to confirm the formation of SCPg-AI-NCs using UV–vis spectrophotometer (Shimadzu-1700, Japan). The absorbance of the formulated SCPg-AI-NCs were assessed at 400–1000 nm wavelengths.

The SCPg-AI-NCs were assessed by the photoluminescence spectroscopic assay and the spectral analysis were done at 350–550 nm wavelength.

The XRD analysis of SCPg-AI-NCs were assessed using ARL EQUINOX 3000 X-ray diffractometer with Cu k-α radiation (λ = 1.5412 Å) in the scanning range of 100–800.

The FT-IR analysis of SCPg-AI-NCs were done using FT-IR apparatus (Cary 630, Agilent Technology, USA) to detect the functional groups bound on the SCPg-AI-NCs. The spectral study was done at 4000–500 cm^{-1}.

The SCPg-AI-NCs were assessed by SEM with DLS studies to scrutinize the size, appearance, and components of the SCPg-AI-NCs. The SCPg-AI-NCs were scrutinized by using Carl Zeiss Ultra-55 FE-SEM apparatus. The SCPg-AI-NCs samples were prepared and placed on a glass slide, dispersed uniformly, and vacuum desiccated to examine by using SEM machine equipped with EDX.

The distribution patterns and average size of formulated SCPg-AI-NCs were examined by using Zeta sizer DLS apparatus (Malvern, USA).

2.4. Experimental rats

The adult wistar albino rats weighing above 180–210 g bodyweight was designated in this work and rats were purchased from the institutional animal facility. All rats were caged on the infection-free polypropylene confines and maintained under laboratory environments with 24 ± 5 °C temperature, 40–70% air humidity, and 12-h light/dark sequence. Rats were permitted freely to get the standard diet and clean drinking water. All rats were adapted for a week in a laboratory before the commencement of experiments.

2.5. Induction of DEN-induced liver cancer

A single carcinogenic dose of DEN (200 mg/kg b.wt in 0.9% saline, i.p.) was injected to the experimental rats on the 8th day of experiment to provoke the liver cancer. Following the retrieval period of 3 weeks, the DEN-injected rats were managed with 0.05% of phenobarbital in the diet as a promoter of liver carcinogenesis for 5 days per week until the completion of experiments (16 weeks) (Chakraborty et al., 2007).

2.6. Experimental groups

Followed by the acclimatization period, all rats were allocated arbitrarily into four groups with six rats in each. Group-I rats were set as a control group. Group-II rats were injected with 200 mg/kg of DEN (as described above) to induce the liver cancer. The group-III rats were treated with 10 mg/kg of formulated SCPg-AI-NCs through oral route an hour before the DEN-injection for 16 consecutive weeks. Group-IV rats were treated with 10 mg/kg of SCPg-AI-NCs alone for 16 weeks without DEN injection. Throughout the experiments, bodyweight of experimental rats were assessed on alternative days. Followed by the completion of experimental period, experimental rats were anesthetized using ketamine/xylazine and sacrificed by cervical dislocation. The serum was prepared using collected blood samples and used for biochemical assays. The liver tissues were excised from the experimental rats and used for the additional assays.

2.7. Quantification of 8-hydroxy-2′ -deoxyguanosine (8-OHdG), total protein, albumin, and globulin contents

The contents of 8-OHdG, globulin, total protein, and albumin in the serum of control and experimental rats were examined with the aid of marker specific assay kits according to the instructions suggested by the manufacturer (Mybiosource, USA).

2.8. Measurement of oxidative stress and antioxidant biomarkers

The TBARS level in the control and experimental rats were studied by using previous method described by Ohkawa et al. (1979). The activities of SOD, CAT, GPx, and GR were studied by using assay kits. The contents of GSH, vitamin-E, and vitamin-C in the serum samples were examined using marker specific kits. All the assays were done in triplicates using the guidelines described by the manufacturer (Thermofisher Scientific, USA).

2.9. Detection of liver marker enzyme activities and tumor marker levels

The liver marker enzyme activities such as alkaline phosphatase (ALP), alanine transaminase (ALT), aspartate transaminase (AST), gamma-glutamyl transferase (GGT), and lactate dehydrogenase (LDH) in the serum of control and experimental rats were examined using respective kits as per the instructions of the manufacturer (Biocompare, USA).

The levels of alpha fetoprotein (AFP) and carcinoembryonic antigen (CEA) in the serum of experimental rats were detected using the assay kits by the manufacturer's guidelines (R&D Systems, Minneapolis, USA).

2.10. Assessment of apoptotic markers

The liver portions were removed from the experimental rats and cleansed with the ice-cold saline. Then liver tissues were homogenized in ice-cold sterile buffered saline and centrifuged at 12,000 rpm for 15 min; the resultant supernatant was collected and used for the assays. The level of Bax, Bcl-2 and activities of caspase-3 & −9 enzymes in the liver tissue homogenates were examined using respective kits by using manufacturer instructions (Mybiosource, USA).

2.11. Histopathological analysis

The liver tissues from the control and treated rats were removed, cleansed with buffer, and processed with 10% of neutral formalin. Then tissues were dehydrated with the addition of graded ethanol and then embedded in a paraffin wax. The paraffinized tissues were sliced into pieces at 5 μm size, deparaffinised, and then stained by using hematoxylin and eosin. The histological changes in the liver tissues were inspected beneath the optical microscope.

2.12. In vitro assays

2.12.1. Cytotoxicity assay

The influence of formulated SCPg-AI-NCs on the viability of liver cancer (HepG2) and normal liver (HL7702) cells were scrutinized using MTT assay. For this, cells were loaded separately onto the 96-wellplate and incubated at 37 °C for 24 h. Then cells were administered with different concentrations of SCPg-AI-NCs (0.5, 1, 2.5, 5, 7.5, & 10 μg) and incubated for 24 h at 37 °C. After that, the MTT reagent was mixed to each wells and further incubated for additional 4 h at 37 °C. After that, 100 μl of DMSO was mixed to all wells to liquefy the formed formazan crystals. Finally, absorbance was taken at 570 nm using microplate reader to identify the viability of cells using formula: treated cells (O.D.)/control (O.D.) × 100 (%).

2.13. Dual staining

The level of apoptotic cell death incidences on the control and SCPg-AI-NCs treated HepG2 cells were studied using dual staining.

For this, HepG2 cells were cultured on the 24-wellplate and treated with 5 μg of SCPg-AI-NCs and 2 μg of doxorubicin (DOX: standard drug) for 24 h at 37 °C. Afterward, 100 μg/ml of AO/EB was used to stain the cells for 5 min. Lastly, the fluorescent intensity of the cells were scrutinized under fluorescent microscope.

2.14. Statistical analysis

Data were statistically examined using GraphPad Prism software and results were represented as mean ± SD of three individual assays. All values were scrutinized by the one-way ANOVA and Tukey's post doc assay to determine the differences between groups and significant was fixed at $p < 0.05$ significant.

3. Results

3.1. Uv–visible spectroscopic analysis

The development of SCPg-AI-NCs in the reaction medium was confirmed by using UV–visible spectral study and data were showed in the Fig. 1(A). The various wavelengths ranging from 400 to 1000 nm were used to measure the absorbance of SCPg-AI-NCs. The highest peak was found at the 282 nm that confirms the presence of SCPg-AI-NCs.

3.2. Photoluminescence analysis

The formulated SCPg-AI-NCs were examined by photoluminescence analysis and finding was presented in the Fig. 1(B). The excitation wavelengths of SCPg-AI-NCs were noted by several peaks at 367 nm, 403 nm, 435 nm, and 476 nm, 505 nm, and 538 nm, respectively, which confirms the presence of SCPg-AI-NCs. The 367 nm and 403 nm peaks demonstrates the free exciton of SCPg-AI-NCs. The peaks at 435 nm and 476 nm exhibits the blue-green emissions and interstitial oxygen vacancies of SCPg-AI-NCs showed by peaks at 505 nm and 538 nm.

3.3. SEM and EDX analysis

The morphology and appearance of formulated SCPg-AI-NCs were studied by the SEM analysis and EDX were performed to assess the elemental compositions of SCPg-AI-NCs. As depicted in the Fig. 2(A&B), the SEM images of SCPg-AI-NCs demonstrated the clear morphology with agglomerated surface and tetragonal shapes. The distinctive peaks of EDX study demonstrated the presence of several elements like presence carbon, nitrogen, potassium, oxygen, and selenium, which is demonstrated by the SCPg-AI-NCs.

3.4. XRD analysis

The crystalline nature and purity of the formulated SCPg-AI-NCs were assessed by using XRD study and finding was showed in the Fig. 3(A). The different clear peaks of the SCPg-AI-NCs were noted at (110), (200), (101), (211), (220), (002), (310), (112), (301), (202), and (321), which proves the purity and crystalline nature of SCPg-AI-NCs with face-centered tetragonal arrangements (Fig. 3A).

3.5. Ft-IR analysis

The formulated SCPg-AI-NCs were investigated by FT-IR analysis to detect the functional groups bound on the SCPg-AI-NCs and data was presented in the Fig. 3(B). The FT-IR spectrum of the SCPg-AI-NCs exhibited the different peaks at various frequencies. The peak at 3413 cm-1 shows the band due to the O-H stretching. The presence of the H stretching was indicated by 2948 cm-1 peak. The bending vibrations of C-O and C-H bonds were revealed by different peaks at 1628 cm-1 and 1115 cm-1. The different peaks at 946 cm-1, 841 cm-1, and 637 cm-1 represents the O-H bonds.

3.6. DLS analysis

The distribution patterns and size of the SCPg-AI-NCs were investigated by the DLS analysis and finding was depicted in the Fig. 3(C). The finding from DLS analysis exhibited the clear peak that indicates the size of SCPg-AI-NCs may 390–450 nm.

3.7. Effect of SCPg-AI-NCs on the albumin, total protein, globulin, and 8-OHdG in the control and experimental rats

The albumin, total protein, globulin, and 8-OHdG levels were assessed and findings were represented in the Fig. 4. The DEN-induced rats exhibited the increased 8-OHdG level and decreased the albumin, total protein, and globulin levels when compared with control. The 10 mg/kg of SCPg-AI-NCs treatment substantially decreased 8-OHdG content in the DEN-induced rats. The SCPg-AI-

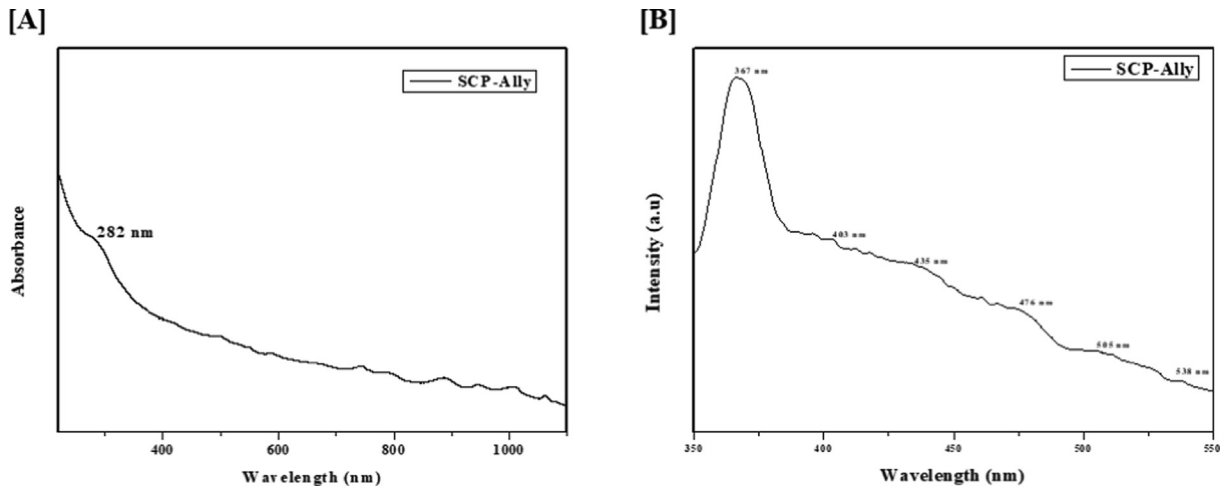

Fig. 1. UV–visible spectroscopy and photoluminescence analysis of SCPg-AI-NCs [A]. UV–Visible spectroscopy study of formulated SCPg-AI-NCs revealed the highest absorption peak at 282 nm. **[B].** Photoluminescence spectral study of formulated SCPg-AI-NCs revealed the excitations at 367 nm, 403 nm, 435 nm, and 476 nm, 505 nm, and 538 nm, respectively.

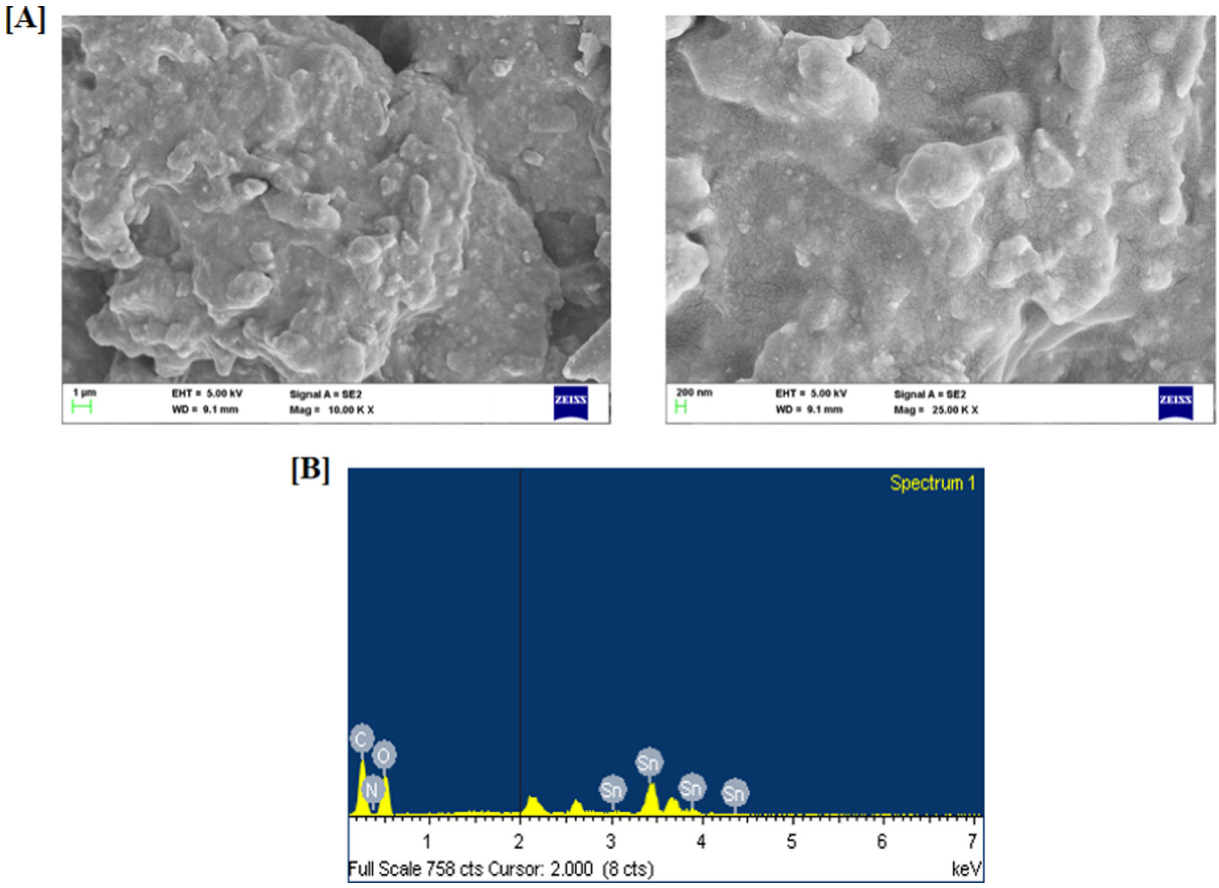

Fig. 2. SEM and DLS analysis of synthesized SCPg-AI-NCs [A]. SEM analysis of formulated SCPg-AI-NCs demonstrates the uneven and dispersed morphological appearance. **[B].** EDX spectral analysis of formulated SCPg-AI-NCs exhibited several peaks that indicates the existence of elements like C, O, N, and Sn.

NCs treatment also improved the contents of albumin, total protein, and globulin in the DEN-induced rats (Fig. 4).

3.8. Effect of SCPg-AI-NCs on the oxidative and antioxidant biomarkers in the control and experimental rats

Fig. 5 exhibits the effect of SCPg-AI-NCs on the oxidative stress and antioxidant biomarkers in both control and experimental rats. The DEN-induced rats exhibited the increased level of TBARS, while decreased GSH, vitamin-E & -C contents. The DEN-induced rats showed the decreased activities of enzymatic antioxidants like CAT, SOD, GPx, and GR. The SCPg-AI-NCs treatment effectively decreased the TBARS and improved the GSH, vitamin-C & -E contents in the DEN-induced rats (Fig. 5). The activities of SOD, GPx, and GR were also improved by the SCPg-AI-NCs treatment in the DEN-induced rats.

3.9. Effect of SCPg-AI-NCs on the liver function marker enzyme activities and tumor marker levels in the control and experimental rats

The effect of SCPg-AI-NCs on the liver function marker enzyme activities and levels of tumor biomarkers were assessed and data were presented in the Fig. 6. The DEN-induced rats exhibited the increased activities of ALT, AST, ALP, LDH, and GGT in the serum when compared with control. The DEN-induction also exhibits the increased contents of AFP and CEA than the control. Interestingly, the SCPg-AI-NCs treatment substantially inhibited those changes in the DEN-challenged liver cancer rats. The activities of ALT, ALP, AST, LDH, and GGT was remarkably decreased by the SCPg-AI-NCs treatment in the DEN-provoked liver cancer rats. The SCPg-AI-NCs treatment also depleted the contents of CEA and AFP in the serum of liver cancer rats (Fig. 6).

3.10. Effect of SCPg-AI-NCs on the apoptotic markers in the control and experimental rats

Fig. 7 demonstrates the effect of SCPg-AI-NCs treatment on the Bax, Bcl-2, and caspases activities. The decreased Bax content and caspase-3 and −9 activities were noted on the DEN-provoked liver cancer rats when compared with control. The DEN-induced rats also exhibited the increased Bcl-2 content. However, the treatment with 10 mg/kg of formulated SCPg-AI-NCs were remarkably increased the Bax content and activities of caspase-3 and −9 in the DEN-challenged liver cancer rats. The SCPg-AI-NCs treatment also diminished the Bcl-2 level in the DEN-induced rats (Fig. 7).

3.11. Effect of SCPg-AI-NCs on the liver histopathology in the control and experimental rats

Fig. 8 exhibits the liver histology of both control and experimental rats. The control rats exhibited the normal tissues structures; while, the liver tissues of DEN-induced cancer rats exhibited the incidences of cirrhosis and tumor nodules. It also demonstrated the dysplastic and the neoplastic nodules. Interestingly, the treatment with the 10 mg/kg of fabricated SCPg-AI-NCs remarkably reduced the DEN-induced dysplasia, neoplasia, and tumor nodules in the DEN-induced rats (Fig. 8).

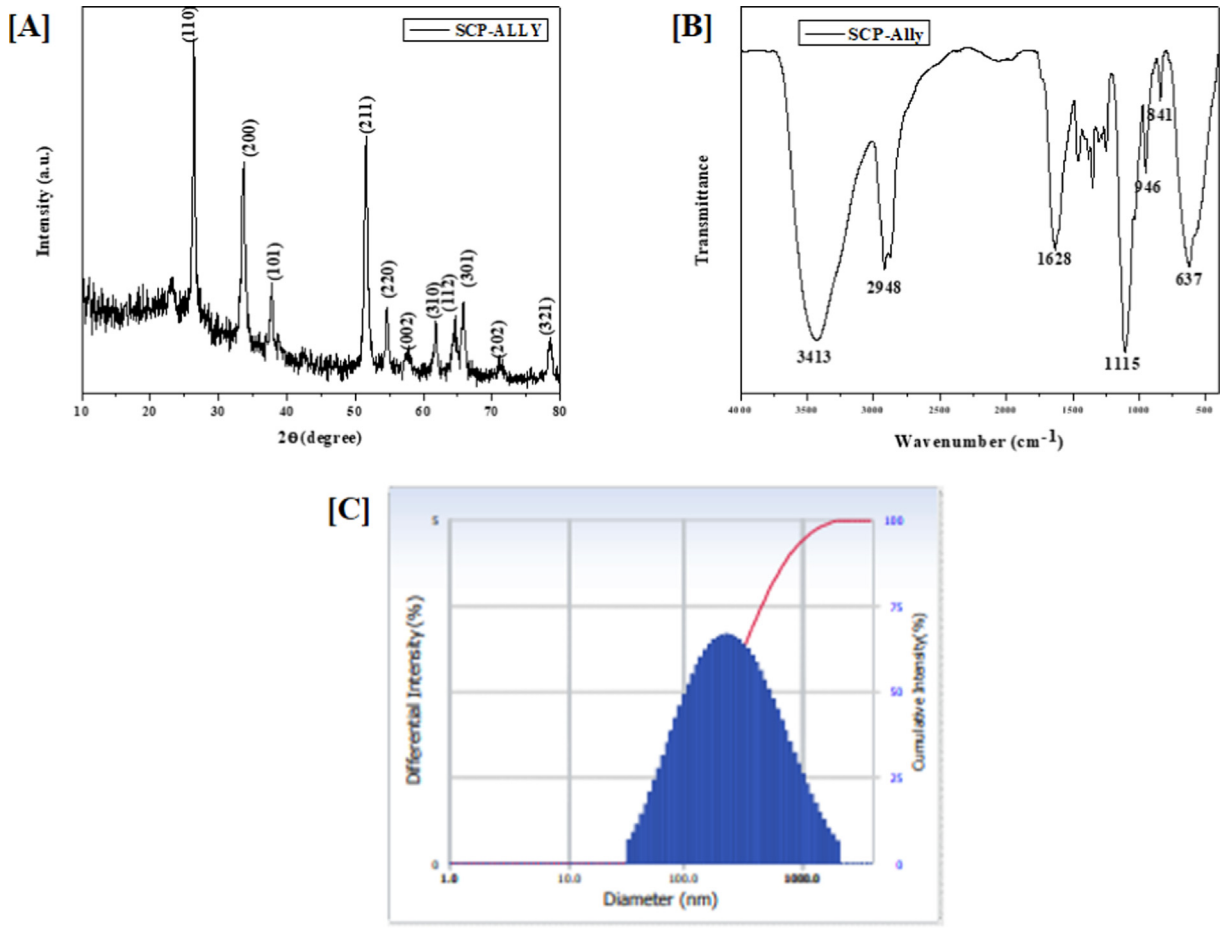

Fig. 3. XRD, FT-IR, and EDX analysis of synthesized SCPg-AI-NCs [A]. XRD analysis revealed the crystallinity of the formulated SCPg-AI-NCs. **[B].** The FT-IR analysis revealed the different peaks at 3413 cm-1, 2948 cm-1, 1628 cm-1, 1115 cm-1, 946 cm-1, 841 cm-1, and 637 cm-1, which proves the existence of several bonding such as hydroxyl (O-H), H, C-O, and C-H bonds on the SCPg-AI-NCs. **[C].** The DLS analysis of formulated CSP-AI-NCs demonstrated the clear peak, which shows a size of SCPg-AI-NCs ranging from 390 to 450 nm with narrowed distribution.

3.12. Effect of SCPg-AI-NCs on the cell viability of Hep-G2 and HL7702 cells

The effects of SCPg-AI-NCs on the cell viability of HepG2 and HL7702 cells were inspected by MTT assay and data were illustrated in the Fig. 9. The SCPg-AI-NCs treatment at various concentrations (0.5–10 μg) were substantially inhibited the viability of HepG2 cells. The treatment with same doses of SCPg-AI-NCs did not showed the cytotoxicity to the normal liver HL7702 cells (Fig. 9). The IC50 of SCPg-AI-NCs for HepG2 cells were found at 5 μg, hence the same dose of SCPg-AI-NCs were selected for additional assays as a IC50 dosage.

3.13. Effect of SCPg-AI-NCs on the apoptotic cell death of Hep-G2 and HL7702 cells

Fig. 10 demonstrates the effect of SCPg-AI-NCs treatment on the apoptotic cell death in the HepG2 cells. The 5 μg of SCPg-AI-NCs treated HepG2 cells exhibited the increased yellow and orange fluorescence than the control cells. These increased fluorescence indicates the presence of early and late apoptotic events in the SCPg-AI-NCs treated HepG2 cells. The 2 μg of DOX treatment also enhanced the apoptosis in the HepG2 cells, which is confirmed by the augmented yellow and orange fluorescence (Fig. 10).

4. Discussion

In recent times, nanotechnology has made several contributions in the field of oncology due to its peculiar properties of diagnosis and drug delivery (Pucci et al., 2019; Krishnan et al., 2017). The developments in the nanotechnology in past decades is remarkably impacting the field of medicine (Chi et al., 2012). Nanomedicine is an rapidly growing field of nanotechnology, which achieves nanostructured or nanoscale materials in medicine to attain ideal medical purposes (Wagner et al., 2006). A nanomedicine usually consists of two compartments namely, the delivery system and a therapeutic agents. A several therapeutic candidates can be loaded in nanomedicines, such as small DNAs/RNAs for gene therapy and drug molecules for chemotherapy, which indicates the multipurpose applications of nanomedicines in several therapies (Haute and Berlin, 2017). At present, the abundant nanomedicines for liver cancer treatment are being developed that would positively offer an alternative strategies to fully accomplish the liver cancer problems in the future (Jiang et al., 2019).

The lack of selective cytotoxicity to the tumor cells is a well-known disadvantage of cancer chemotherapy, which leads to considerable damage to the normal cells. Additionally, these strategies often experienced with several deleterious adverse effects, which substantially decrease the life quality of survived individuals (Amiri et al., 2019). The utilization of nanocomposites as drug delivery systems has a efficacy to solve the several side effects trig-

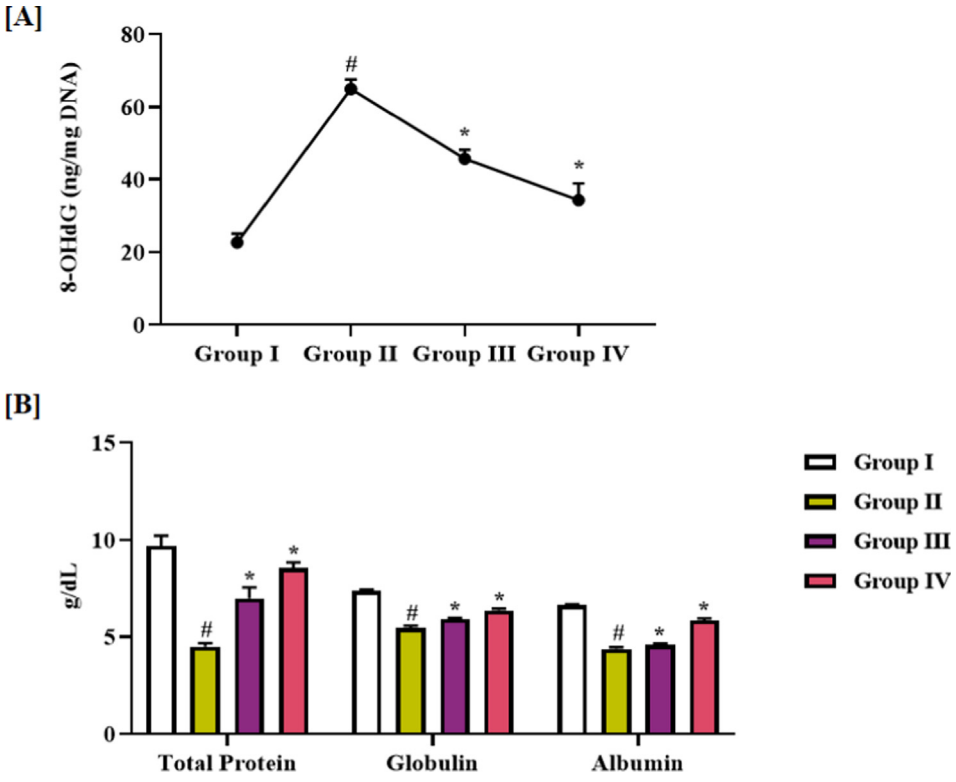

Fig. 4. Effect of SCPg-AI-NCs on the albumin, total protein, globulin, and 8-OHdG in the control and experimental rats Results are given as a mean ± SD of three separate assays. The data were scrutinized by one-way ANOVA and Tukey's post hoc assay. '#' $p < 0.05$ compared with control '*' $p < 0.01$ compared with DEN-induced rats.

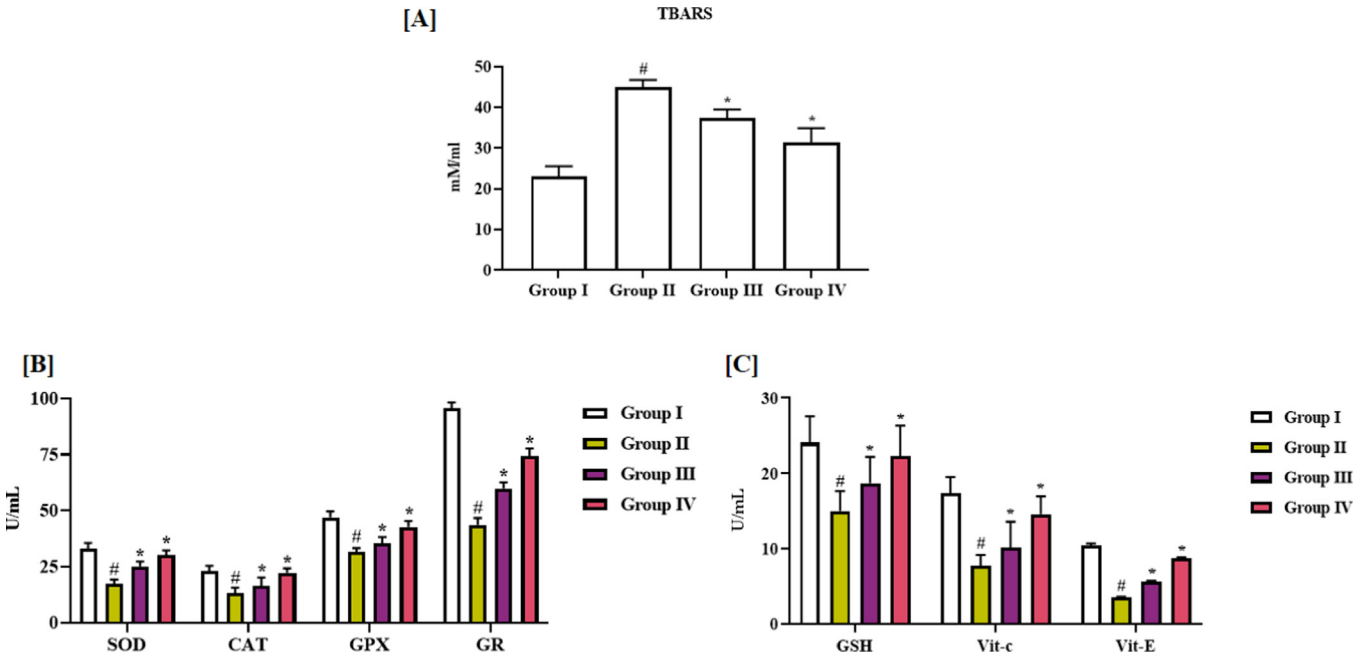

Fig. 5. Effect of SCPg-AI-NCs on the oxidative and antioxidant biomarkers in the control and experimental rats Results are given as a mean ± SD of three separate assays. The data were scrutinized by one-way ANOVA and Tukey's post hoc assay. '#' $p < 0.05$ compared with control '*' $p < 0.01$ compared with DEN-induced rats.

gered by chemotherapeutic drugs to normal cells (Shende and Shah, 2021). It is possible to control the architectures of nanocarriers in that way, it could enhance the targeted local delivery and controlled drug release (Martinelli et al., 2019). Additionally, nanocarriers also has the ability to protect and package of the drug candidates, which was insoluble, unstable, fragile, and toxic for conventional delivery (Saw and Song, 2020). The several nanocarriers are being used as nanocarriers in delivery of nanomedicines for liver cancer therapy comprises polymers, micelles, liposomes, hydrogels, biological, hybrid, and inorganic nanomaterials (Baig et al., 2019). Several efforts have been paid in order to manipulating them as a nanocarriers for nanomedicines to enhance the anti-

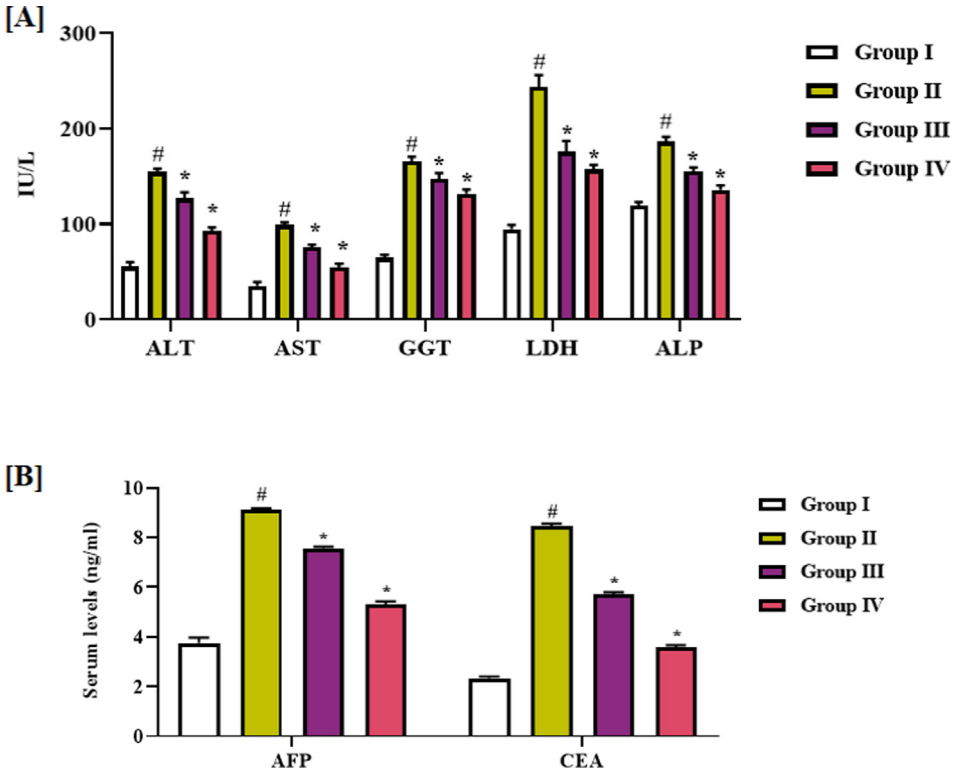

Fig. 6. Effect of SCPg-AI-NCs on the liver function marker enzyme activities and tumor marker levels in the control and experimental rats Results are given as a mean ± SD of three separate assays. The data were scrutinized by one-way ANOVA and Tukey's post hoc assay. '#' $p < 0.05$ compared with control '*' $p < 0.01$ compared with DEN-induced rats.

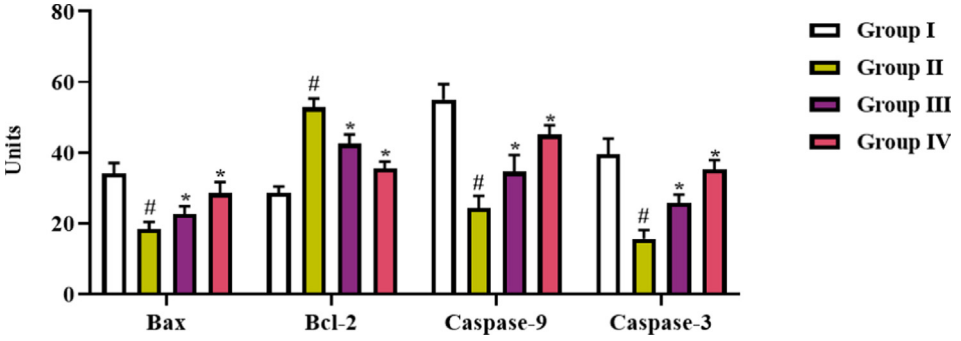

Fig. 7. Effect of SCPg-AI-NCs on the apoptotic markers in the control and experimental rats Results are given as a mean ± SD of three separate assays. The data were scrutinized by one-way ANOVA and Tukey's post hoc assay. '#' $p < 0.05$ compared with control '*' $p < 0.01$ compared with DEN-induced rats.

cancer property and decrease deleterious effects in the liver cancer management (van der Meel et al., 2019). Here, we formulated the SCPg-AI-NCs and assessed its therapeutic potential against the DEN-induced liver cancer in rats. The findings of various characterization techniques confirmed the formation and presence of SCPg-AI-NCs with tetragonal shape, narrowed distribution, and size ranging from 390 to 450 nm. Our results of characterization studies were supported by the previous reports done by Govindan et al. (2012), Jan et al. (2020), and Nair Nandana et al. (2022).

Liver cancer is a most aggressive solid tumor with increased mortality rates worldwide. Many liver cancer patients are become treatment resistance followed by an long-term therapy (Mohamed et al., 2017). The poor prognosis after the surgery in patients still remains as a major problem (Cai et al., 2017). DEN is a well-established hepatocarcinogen, and it triggers liver damage and is frequently utilized to trigger liver carcinogenesis in animal models (Sklavos et al., 2018). It was reported that pathological process of DEN-induced liver carcinogenesis in found more similar to the patterns of human liver cancer (Kurma et al., 2021). Hence, the DEN-induced animal models of liver cancer is extensively utilized in liver cancer research (Schneider et al., 2012). The current research focused to evaluate the anticancer activity of formulated SCPg-AI-NCs against the DEN-initiated liver carcinogenesis in rats.

During the development of liver cancer, there are many factors play a major roles such as oxidative stress and inflammation, which provokes cirrhosis and liver dysfunction in liver cancer patients (Balaha et al., 2016; Wen et al., 2016). It is well-established that the oxidative stress participates in several phases of tumorigenesis (Patterson et al., 2018). Oxidative stress is described as a condition of disproportion between accumulation of free radicals and endogenous antioxidant protection systems. Such imbalance is tightly connected with the initiation and progression of several chronic ailments, such as cancer (Wang et al., 2016). The endogenous antioxidant protective mechanisms like

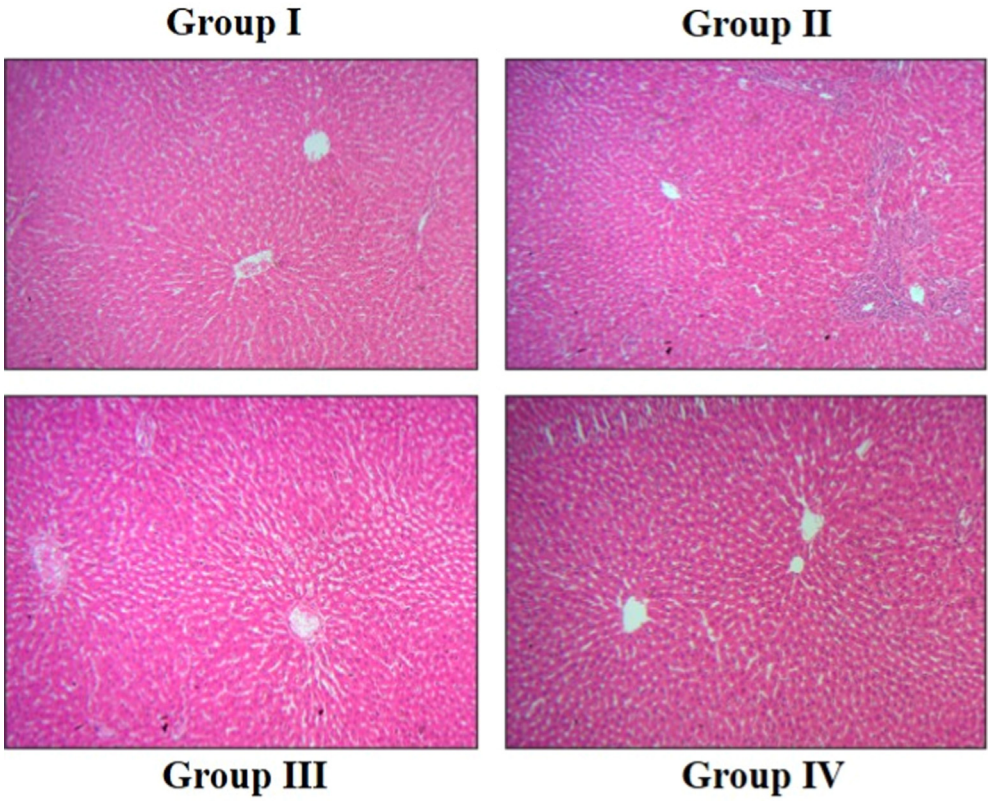

Fig. 8. Effect of SCPg-AI-NCs on the liver histopathology in the control and experimental rats The normal histological structures and hepatocytes arrangements without lesions and changes were observed in the control and 10 mg/kg of formulated SCPg-AI-NCs alone treated rats **(Group I and IV)**. The liver tissues of DEN-challenged rats exhibited dysplastic and neoplastic nodules and tumor incidences **(Group II)**. The 10 mg/kg of formulated SCPg-AI-NCs remarkably attenuated the DEN-provoked histological alterations **(Group III)**.

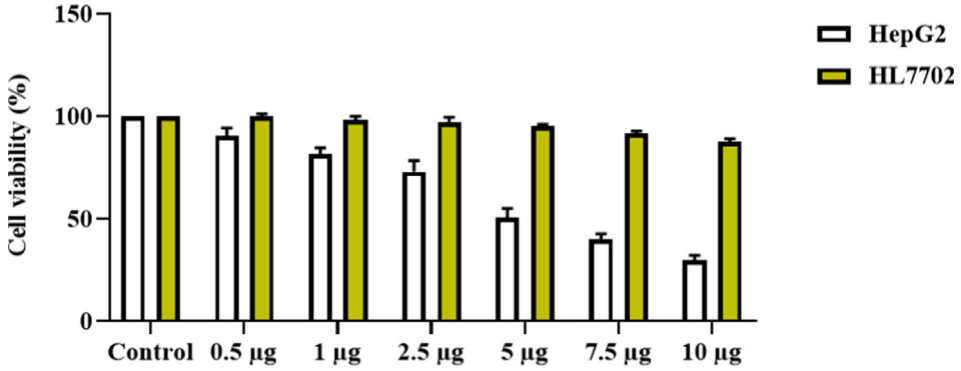

Fig. 9. Effect of SCPg-AI-NCs on the cell viability of Hep-G2 and HL7702 cells The formulated SCPg-AI-NCs treated HepG2 cells at various doses 0.5–10 µg remarkably inhibited the viability of HepG2 cells and the same doses of SCPg-AI-NCs did not affected the normal liver HL7702 cells. Results are given as a mean ± SD of three separate assays. The data were scrutinized by one-way ANOVA and Tukey's post hoc assay. *values does not share common superscript and significantly varied from control.

SOD, CAT, GPx, and GR guards the liver tissues from the oxidative damage (Kumar et al., 2012). SOD is a most vital antioxidant enzyme that counteracts adverse effects of free radicals (Anwar and Younus, 2017). GR is a critical player of cellular defense against oxidative stress by inhibiting the accretion of oxidized glutathione and hence regulating the redox balance (Al-Seeni et al., 2016). GSH performs an imperative function against lipid peroxidation and acts as a co-factor for GPx. GPx is a selenium-consisting antioxidant enzyme, which is a second line defense against hydroperoxides by catalyzing the reduction of lipid peroxides and H_2O_2 to lipid alcohols and water (Shaban et al., 2014). The other antioxidants such as SOD, GSH, and CAT protect the cells/tissues from the adverse effects of free radicals (Kurutas, 2015). Here, we found that the DEN-induced rats demonstrated the increased TBARS level and decreased GSH, vitamin-C & -E levels in the serum. DEN-induced rats also showed the decreased SOD, CAT, GPx, and GR activities. Interestingly, the treatment with the 10 mg/kg of formulated SCPg-AI-NCs substantially improved the GSH, vitamin-C & -E contents. SCPg-AI-NCs also increased the activities of SOD, CAT, GPx, and GR in the DEN-provoked rats. The current findings were supported by the previous study, which reported that the DEN-induced animals showed the decreased antioxidants such as GSH, GST, and SOD concentrations (Alsahli et al., 2021).

A previous literature highlighted that the DEN administration alters the activities of liver function marker enzymes and possesses hepatotoxicity (Khan et al., 2017). It is well-established that the

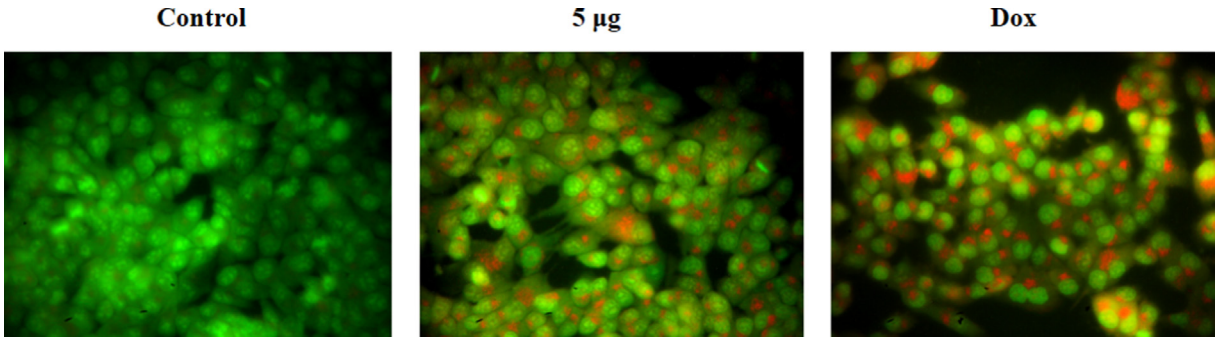

Fig. 10. Effect of SCPg-AI-NCs on the cell viability of Hep-G2 and HL7702 cells The 5 µg of synthesized SCPg-AI-NCs treated HepG2 cells demonstrated the elevated yellow and orange fluorescence than control, which confirms the early and late phases of apoptosis.

metabolism of several drugs and chemicals are takes place in the liver, which makes it highly vulnerable to the chemicals and drugs-induced toxicity. Therefore, these chemicals and drugs induce liver injury and change the hepatocyte arrangements. The augmented activities of liver marker enzymes in the serum are connected with liver injury due to the damages in the hepatic cells, which leads to the release of these enzymes into blood flow (Breikaa et al., 2014). AST and ALT are primarily found in the liver cells, and its release is connected with cell damages (Wang et al., 2015). The considerable elevation in AST, ALT, and ALP can be utilized as a biomarkers to diagnose the chemicals and drugs-triggered alterations in the liver function (Mansouri et al., 2018). The present findings revealed that DEN-provoked rats demonstrated the improved activities of ALP, AST, ALT, LDH, and GGT. Whereas, the treatment with 10 mg/kg of formulated SCPg-AI-NCs considerably decreased the ALP, AST, ALT, LDH, and GGT activities in a serum of DEN-challenged rats. A previous report by Saleem et al. (2020) found that the serum activities of ALT, AST, and GGT enzymes were amplified in the DEN-induced rats, which supported our current findings.

Apoptosis is a crucial player of cell death regulation, and evasion from apoptosis is a vital cause of tumor cell survival (Fabregat et al., 2007). The equilibrium between cell growth and apoptosis is important for the structural and functional maintenance of normal cells/tissues. The initiation of cancer development may because of the suppression of normal apoptotic event, which causes the disproportion between cell growth and death. Indeed, apoptosis provides a tissue defense against carcinogens via inhibiting the survival of genetically altered cells. Consequently, apoptosis inhibition was explicated as a dominant factor of promotion of liver cancer in several animal models (Li et al., 2013). The evasion of apoptosis is a critical factor of tumorigenesis, which facilitates to the uncontrolled cell growth. The ability of tumor cells to inhibit the apoptosis may increase the cell growth and makes them as immortal cell colonies, which are usually known as tumors. The flaws in apoptosis is a vital factor of treatment resistance and increasing the tumor life threshold. Hence, the stimulation of apoptosis in cancer cells is believed to be a promising strategy to eradicate the tumors (Fandy et al., 2014). The current findings suggested that the SCPg-AI-NCs treatment substantially repressed the cell growth and triggered apoptotic cell death in the HepG2 cells.

The cancer cells usually undergo numerous molecular events to evade apoptosis and gain resistance to apoptotic factors via enhancement of anti-apoptotic gene expressions e.g., Bcl-2 or inhibition of pro-apoptotic gene expression e.g., Bax (Hassan et al., 2014). The anti-apoptotic genes such as Bcl-2 defend the cells from apoptosis and maintains normal functions, while pro-apoptotic genes like Bad, Bax, and Bid are triggered by DNA injury and cellular stress (Wong, 2011; Danial, 2007). Bcl-2 and Bax have received more attention because of their participation in the cell apoptosis regulation (Cory and Adams, 2002). Bcl-2 and Bax are a set of negative-positive apoptosis controlling proteins. Hence, it was clear that the cell apoptosis incidence is connected with the disproportion of Bax and Bcl 2 levels. It was already highlighted that the apoptosis inhibition plays a major roles in the cancer progression (Sia et al., 2017). The findings of this investigation exhibited that the level of Bcl-2 was found elevated and Bax level was reduced in the DEN-challenged liver cancer rats. Interestingly, the SCPg-AI-NCs treatment substantially decreased the Bcl-2 level and improved the Bax level in the DEN-induced rats. Caspases are a family of protease enzymes, which plays a major roles in the commencement and regulation of cell apoptosis. Generally, caspases are participates in a cellular apoptosis in two categories namely effectors (caspase-3, −6, and −7) and initiators (caspase-8, −9, and −10) (McComb et al., 2019). Caspases alter the expressions of pro- and anti-apoptotic proteins, when they activated, thus leading to apoptosis (Poreba et al., 2019). Here, our findings exhibited that the activities of caspase-3 and −9 were decreased in the DEN-induced rats. However, the treatment with SCPg-AI-NCs remarkably improved the activities of caspase-3 and −9 in the DEN-challenged rats. Our present findings were supported by the previous research report done by Punvittayagul et al. (2021).

The assessment of CEA content in serum is clinically reliable and beneficial marker for the diagnosis of tumorigenesis. A considerable augmentation in the CEA content is a prognostic marker of the state of tumorigenesis (Thomas et al., 2015). The overexpression of CEA is tightly connected with the tumor metastasis (Pakdel et al., 2016). It was already reported that the CEA has been over-expressed in several types of human cancers (Sauzay et al., 2016). The tight connection between CEA expression and cancers has encouraged the utilization of CEA as a cancer biomarker (Tiernan et al., 2013). AFP is a valuable diagnostic tumor maker of liver cancer that has been utilized extensively for diagnosis, monitoring, tumor staging, and even predicting the liver cancer reappearance (Gani et al., 2019). Additionally, the increased levels of AFP in the serum has been well reported in the liver cancer (Galle et al., 2019). A previous report found that the AFP plays a major roles during the tumor growth and can trigger the cancer cell proliferation (Chen et al., 2020). In similar manner, here our findings demonstrated that the DEN-induced liver cancer rats exhibited the increased CEA and AFP contents. Whereas, the contents of CEA and AFP was appreciably decreased by the SCPg-AI-NCs treatment. A previous report by Anwar et al. (2021) reported that the DEN-induced animals showed that the level of AFP and CEA was found increased than control, which supported the findings of this study.

5. Conclusion

The findings of this research work suggests that formulated SCPg-AI-NCs treatment attenuates the liver cancer by inhibiting oxidative stress response in the DEN-induced rat liver cancer model. The treatment with SCPg-AI-NCs substantially improved the apoptotic markers such as Bax, caspase-3, and capsase-9 and reduced the Bcl-2 in the DEN-induced rats. The *in vitro* findings also proved that the SCPg-AI-NCs treatment inhibited cell viability and stimulated apoptosis in the HepG2 cells. These results proposed that SCPg-AI-NCs can be a promising anticancer nano-drug in the future to treat the liver carcinogenesis. However, the further investigations still required in the future for the clear understanding of the underlying molecular mechanisms of the SCPg-AI-NCs against liver cancer.

Declaration of Competing Interest

The authors declare that they have no known competing financial interests or personal relationships that could have appeared to influence the work reported in this paper.

Acknowledgement

This project was supported by Researchers Supporting Project number (RSP-2021/230) King Saud University, Riyadh, Saudi Arabia.

References

Alsahli, M.A., Almatroodi, S.A., Almatroudi, A., Khan, A.A., Anwar, S., Almutary, A.G., Alrumaihi, F., Rahmani, A.H., Roscetto, E., 2021. 6-Gingerol, a major ingredient of ginger attenuates diethylnitrosamine-induced liver injury in rats through the modulation of oxidative stress and anti-inflammatory activity. Mediators Inflamm. 2021, 1–17.

Al-Seeni, M.N., El Rabey, H.A., Zamzami, M.A., Alnefayee, A.M., 2016. The hepatoprotective activity of olive oil and Nigella sativa oil against CCl4 induced hepatotoxicity in male rats. BMC Complement. Altern. Med. 16, 438.

Amiri, M., Salavati-Niasari, M., Akbari, A., 2019. Magnetic nanocarriers: evolution of spinel ferrites for medical applications. Adv. Colloid Interface Sci. 265, 29–44.

Anwar, H., Moghazy, A., Osman, A., Abdel Rahman, A., 2021. The therapeutic effect of myrrh (commiphora molmol) and doxorubicin on diethylnitrosamine induced hepatocarcinogenesis in male albino rats. Asian Pac J Cancer Prev. 22 (7), 2153–2163.

Anwar, S., Younus, H., 2017. Antiglycating potential of ellagic acid against glucose and methylglyoxal induced glycation of superoxide dismutase. J. Protein Proteomics 8 (1), 1–12.

Baig, B., Halim, S.A., Farrukh, A., Greish, Y., Amin, A., 2019. Current status of nanomaterial-based treatment for hepatocellular carcinoma. Biomed. Pharmacother. 116, 108852. https://doi.org/10.1016/j.biopha.2019.108852.

Balaha, M., Kandeel, S., Barakat, W., 2016. Carvedilol suppresses circulating and hepatic IL-6 responsible for hepatocarcinogenesis of chronically damaged liver in rats. Toxicol. Appl. Pharmacol. 311, 1–11.

Barahuie, F., Hussein, M.Z., Hussein-Al-Ali, S.H., Arulselvan, P., Fakurazi, S., Zainal, Z., 2013. Preparation and controlled-release studies of a protocatechuic acid-magnesium/aluminum-layered double hydroxide nanocomposite. Int. J. Nanomed. 8, 1975–1987.

Bhattacharya, A., Tang, L., Li, Y., Geng, F., Paonessa, J.D., Chen, S.C., Wong, M.K., Zhang, Y., 2010. Inhibition of bladder cancer development by allyl isothiocyanate. Carcinogenesis 31, 281–286.

Bray, F., Ferlay, J., Soerjomataram, I., Siegel, R.L., Torre, L.A., Jemal, A., 2018. Global cancer statistics 2018: GLOBOCAN estimates of incidence and mortality worldwide for 36 cancers in 185 countries. CA Cancer J. Clin. 68 (6), 394–424.

Breikaa, R.M., Algandaby, M.M., El-Demerdash, E., Abdel-Naim, A.B., 2014. Biochanin A protects against acute carbon tetrachloride-induced hepatotoxicity in rats. Biosci. Biotechnol. Biochem. 77, 909–916.

Cai, H., Zhu, X.-D., Ao, J.-Y., Ye, B.-G., Zhang, Y.-Y., Chai, Z.-T., Wang, C.-H., Shi, W.-K., Cao, M.-Q., Li, X.-L., Sun, H.-C., 2017. Colonystimulating factor-1-induced AIF1 expression in tumor associated macrophages enhances the progression of hepatocellular carcinoma. Oncoimmunology 6 (9), e1333213. https://doi.org/10.1080/2162402X.2017.1333213.

Chakraborty, T., Chatterjee, A., Rana, A., Srivastawa, S., Damodaran, S., Chatterjee, M., 2007. Cell proliferation and hepatocarcinogenesis in rat initiated by diethyl nitrosamine and promoted by phenobarbital: potential roles of early DNA damage and liver metallothionein expression. Life Sci. 81 (6), 489–499.

Chang, P.-Y., Tsai, F.-J., Bau, D.-T., Hsu, Y.-M., Yang, J.-S., Tu, M.-G., Chiang, S.-L., 2021. Potential effects of allyl isothiocyanate on inhibiting cellular proliferation and inducing apoptotic pathway in human cisplatin-resistant oral cancer cells. J. Formos Med. Assoc. 120 (1), 515–523.

Chen, T., Dai, X., Dai, J., Ding, C., Zhang, Z., Lin, Z., Hu, J., Lu, M., Wang, Z., Qi, Y., Zhang, L., Pan, R., Zhao, Z., Lu, L., Liao, W., Lu, X., 2020. AFP promotes HCC progression by suppressing the HuR-mediated Fas/FADD apoptotic pathway. Cell Death Dis. 11, 822.

Chi, X.Q., Huang, D.T., Zhao, Z.H., Zhou, Z.J., Yin, Z.Y., Gao, J.H., 2012. Nanoprobes for in vitro diagnostics of cancer and infectious diseases. Biomaterials 33, 189–206.

Cory, S., Adams, J.M., 2002. The Bcl2 family: regulators of the cellular life-or-death switch. Nat. Rev. Cancer 2 (9), 647–656.

Danial, N.N., 2007. BCL-2 family proteins: critical checkpoints of apoptotic cell death. Clin. Cancer Res. 13, 7254–7263.

Fabregat, I., Roncero, C., Fernandez, M., 2007. Survival and apoptosis: a dysregulated balance in liver cancer. Liver Int. 27, 155–162.

Fandy, T.E., Jiemjit, A., Thakar, M., Rhoden, P., Suarez, L., Gore, S.D., 2014. Decitabine induces delayed reactive oxygen species (ROS) accumulation in leukemia cells and induces the expression of ROS generating enzymes. Clin. Cancer Res. 20 (5), 1249–1258.

Galle, P.R., Foerster, F., Kudo, M., Chan, S.L., Llovet, J.M., Qin, S., Schelman, W.R., Chintharlapalli, S., Abada, P.B., Sherman, M., Zhu, A.X., 2019. Biology and significance of alpha-fetoprotein in hepatocellular carcinoma. Liver Int. 39 (12), 2214–2229.

Gani, S.A., Muhammad, S.A., Kura, A.U., Barahuie, F., Hussein, M.Z., Fakurazi, S., Sheweita, S.A., 2019. Effect of protocatechuic acid-layered double hydroxide nanoparticles on diethylnitrosamine/phenobarbital-induced hepatocellular carcinoma in mice. PLoS ONE 14 (5), e0217009. https://doi.org/10.1371/journal.pone.0217009.

Govindan, S., Nivethaa, E.A.K., Saravanan, R., Narayanan, V., Stephen, A., 2012. Synthesis and characterization of chitosan–silver nanocomposite. Appl. Nanosci. 2 (3), 299–303.

Hassan, M., Watari, H., AbuAlmaaty, A., Ohba, Y., Sakuragi, N., 2014. Apoptosis and molecular targeting therapy in cancer. Biomed. Res. Int. 2014, 1–23.

Haute, D.V., Berlin, J.M., 2017. Challenges in realizing selectivity for nanoparticle biodistribution and clearance: lessons from gold nanoparticles. Ther. Deliv. 8 (9), 763–774.

Hwang, E.-S., Kim, G.H., 2009. Allyl isothiocyanate influences cell adhesion, migration and metalloproteinase gene expression in SK-Hep1 cells. Exp. Biol. Med. (Maywood) 234 (1), 105–111.

Ikeda, K., 2019. Recent advances in medical management of hepatocellular carcinoma. Hepatol. Res. 49 (1), 14–32.

Jan, H., Shah, M., Usman, H., Khan, M.A., Zia, M., Hano, C., Abbasi, B.H., 2020. Biogenic synthesis and characterization of antimicrobial and antiparasitic zinc oxide (ZnO) nanoparticles using aqueous extracts of the himalayan columbine (Aquilegia pubiflora). Front. Mater.

Jiang, X., Du, B., Zheng, J., 2019. Glutathione-mediated biotransformation in the liver modulates nanoparticle transport. Nat. Nanotechnol. 14, 874–882.

Khan, F., Khan, T.J., Kalamegam, G., Pushparaj, P.N., Chaudhary, A., Abuzenadah, A., Kumosani, T., Barbour, E., Al-Qahtani, M., 2017. Anti-cancer effects of Ajwa dates (Phoenix dactylifera L.) in diethylnitrosamine induced hepatocellular carcinoma in Wistar rats. BMC Compl. Alternative Med. 17, 418.

Kim, M.W., Choi, S., Kim, S.Y., Yoon, Y.S., Kang, J.-H., Oh, S.H., 2018. Allyl isothiocyanate ameliorates dextran sodium sulfate-induced colitis in mouse by enhancing tight junction and mucin expression. Int. J. Mol. Sci. 19, 2025.

Krishnan, P., Rajan, M., Kumari, S., Sakinah, S., Priya, S.P., Amira, F., Danjuma, L., Pooi Ling, M., Fakurazi, S., Arulselvan, P., Higuchi, A., Arumugam, R., Alarfaj, A.A., Munusamy, M.A., Hamat, R.A., Benelli, G., Murugan, K., Kumar, S.S., 2017. Efficiency of newly formulated camptothecin with β-cyclodextrin-EDTA-Fe3O4 nanoparticle-conjugated nanocarriers as an anti-colon cancer (HT29) drug. Sci. Rep. 7 (1), 10962.

Kumar, M., Sharma, V.L., Sehgal, A., Jain, M., 2012. Protective effects of green and white tea against benzo(a)pyrene induced oxidative stress and DNA damage in murine model. Nutr. Cancer 64 (2), 300–306.

Kurma, K., Manches, O., Chuffart, F., Sturm, N., Gharzeddine, K., Zhang, J., Mercey-Ressejac, M., Rousseaux, S., Millet, A., Lerat, H., Marche, P.N., Jilkova, Z.M., Decaens, T., 2021. DEN-induced rat model reproduces key features of human hepatocellular carcinoma. Cancers (Basel) 13 (19), 4981.

Kurutas, E.B., 2015. The importance of antioxidants which play the role in cellular response against oxidative/nitrosative stress: current state. Nutr. J. 15, 1–22.

Lai, K.C., Lu, C.C., Tang, Y.J., Chiang, J.H., Kuo, D.H., Chen, F.A., Chen, I.L., Yang, J.S., 2014. Allyl isothiocyanate inhibits cell metastasis through suppression of the MAPK pathways in epidermal growth factor-stimulated HT29 human colorectal adenocarcinoma cells. Oncol. Rep. 31, 189–196.

Lata, S., Sharma, G., Joshi, M., Kanwar, P., Mishra, T., 2017. Role of nanotechnology in drug delivery. Int. J. Nanotechnol. Nanosci. 5, 1–29.

Li, J., Cai, C., Sun, T., Wang, L., Wu, H., Yu, G., 2018. Chitosan-based nanomaterials for drug delivery. Molecules 23, 2661.

Li, Y., Chen, L., Chan, T.H., Liu, M., Kong, K.L., Qiu, J.L., Li, Y., Yuan, Y.F., Guan, X.Y., 2013. SPOCK1 is regulated by CHD1L and blocks apoptosis and promotes HCC cell invasiveness and metastasis in mice. Gastroenterology 144, 179–191.

Liccioni, A., Reig, M., Bruix, J., 2014. Treatment of hepatocellular carcinoma. Dig. Dis. Basel Switz. 32, 554–563.

Lu, H., Wang, J., Wang, T., Zhong, J., Bao, Y., Hao, H., 2016. Recent progress on nanostructures for drug delivery applications. J. Nanomater. 2016, 20.

Mansouri, A., Gattolliat, C.H., Asselah, T., 2018. Mitochondrial dysfunction and signaling in chronic liver diseases. Gastroenterology 155 (3), 629–647.
Martinelli, C., Pucci, C., Ciofani, G., 2019. Nanostructured carriers as innovative tools for cancer diagnosis and therapy. APL. Bioeng. 3, 011502.
McComb, S., Chan, P.K., Guinot, A., et al., 2019. Efficient apoptosis requires feedback amplification of upstream apoptotic signals by effector caspase-3 or-7. Sci. Adv. 5, eaau9433.
Meng, F., Sun, Y., Lee, R.J., Wang, G., Zheng, X., Zhang, H., Fu, Y., Yan, G., Wang, Y., Deng, W., Parks, E., Kim, B.Y.S., Yang, Z., Jiang, W., Teng, L., 2019. Folate receptor-targeted albumin nanoparticles based on microfluidic technology to deliver cabazitaxel. Cancers 11 (3), 1571.
Milewska, S., Niemirowicz-Laskowska, K., Siemiaszko, G., Nowicki, P., Wilczewska, A.Z., Car, H., 2021. Current trends and challenges in pharmacoeconomic aspects of nanocarriers as drug delivery systems for cancer treatment. Int. J. Nanomed. 16, 6593–6644.
Mintz, K.J., Leblanc, R.M., 2021. The use of nanotechnology to combat liver cancer: progress and perspectives. Biochim. Biophys. Acta Rev. Cancer 1876, (2) 188621.
Mohamed, M.S., Bishr, M.K., Almutairi, F.M., Ali, A.G., 2017. Inhibitors of apoptosis: clinical implications in cancer. Apoptosis 22, 1487–1509.
Nair Nandana, C., Christeena, M., Bharathi, D., 2022. Synthesis and characterization of chitosan/silver nanocomposite using rutin for antibacterial, antioxidant and photocatalytic applications. J. Cluster Sci. 33, 269–279.
Ohkawa, H., Ohishi, N., Yagi, K., 1979. Assay for lipid peroxides in animal tissues by thiobarbituric acid reaction. Anal. Biochem. 95, 351–358.
Olivier, C., Vaughn, S.F., Mizubuti, E.S., Loria, R., 1999. Variation in allyl isothiocyanate production within Brassica species and correlation with fungicidal activity. J. Chem. Ecol. 25, 2687–2701.
Pakdel, A., Malekzadeh, M., Naghibalhossaini, F., 2016. The association between preoperative serum CEA concentrations and synchronous liver metastasis in colorectal cancer patients. Cancer Biomarkers 16 (2), 245–252.
Palazzolo, S., Bayda, S., Hadla, M., Caligiuri, I., Corona, G., Toffoli, G., et al., 2018. The clinical translation of organic nanomaterials for cancer therapy: a focus on polymeric nanoparticles, micelles, liposomes and exosomes. Curr. Med. Chem. 25, 4224–4268.
Patterson, A.D., Gonzalez, F.J., Perdew, G.H., Peters, J.M., 2018. Molecular regulation of carcinogenesis: friend and foe. Toxicol. Sci. 165, 277–283.
Poreba, M., Groborz, K., Navarro, M., et al., 2019. Caspase selective reagents for diagnosing apoptotic mechanisms. Cell Death Differ. 26, 229–244.
Pucci, C., Martinelli, C., Ciofani, G., 2019. Innovative approaches for cancer treatment: current perspectives and new challenges. Ecancermedicalscience 13, 961.
Punvittayagul, C., Chariyakornkul, A., Jarukamjorn, K., Wongpoomchai, R., 2021. Protective role of vanillic acid against diethylnitrosamine- and 1,2-dimethylhydrazine-induced hepatocarcinogenesis in rats. Molecules 26 (9), 2718.
Qin, G., Li, P., Xue, Z., 2018. Effect of allyl isothiocyanate on the viability and apoptosis of the human cervical cancer HeLa cell line in vitro. Oncol Lett. 15 (6), 8756–8760.
Sahin, N., Orhan, C., Erten, F., Tuzcu, M., Defo Deeh, P.B., Ozercan, I.H., Juturu, V., Kazim, S., 2019. Effects of allyl isothiocyanate on insulin resistance, oxidative stress status, and transcription factors in high-fat diet/streptozotocin-induced type 2 diabetes mellitus in rats. J. Biochem. Mol. Toxicol. 33, e22328.
Saleem, S., Kazmi, I., Ahmad, A., Abuzinadah, M.F., Samkari, A., Alkrathy, H.M., Khan, R., 2020. Thiamin regresses the anticancer efficacy of methotrexate in the amelioration of diethyl nitrosamine-induced hepatocellular carcinoma in wistar strain rats. Nutr. Cancer 72 (1), 170–181.
Sauzay, C., Petit, A., Bourgeois, A.M., Barbare, J.C., Chauffert, B., Galmiche, A., Houessinon, A., 2016. Alpha-foetoprotein (AFP): a multi-purpose marker in hepatocellular carcinoma. Clin. Chim. Acta 463, 39–44.
Savio, A.L., da Silva, G.N., Salvadori, D.M., 2015. Inhibition of bladder cancer cell proliferation by allyl isothiocyanate (mustard essential oil). Mutat Res 771, 29–35.
Saw, P.E., Song, E.W., 2020. siRNA therapeutics: a clinical reality. Sci. China Life Sci. 63, 485–500.
Schneider, C., Teufel, A., Yevsa, T., Staib, F., Hohmeyer, A., Walenda, G., 2012. Adaptive immunity suppresses formation and progression of diethylnitrosamine-induced liver cancer. Gut 61 (12), 1733–1743.
Shaban, N.Z., El-Kersh, M.A.R., Bader-Eldin, M.M., Kato, S.A., Hamoda, A.F., 2014. Effect of Punica granatum (Pomegranate) juice extract on healthy liver and hepatotoxicity induced by diethylnitrosamine and phenobarbital in male rats. J. Med. Food 17, 339–349.
Shaban, N.Z., Aboelsaad, A.M., Shoueir, K.R., Abdulmalek, S.A., Awad, D., Shaban, S.Y., Mansour, H., 2020. Chitosan-based dithiophenolato nanoparticles: preparation, mechanistic information of DNA binding, antibacterial and cytotoxic activities. J. Mol. Liq. 318, 114252.
Shende, P., Shah, P., 2021. Carbohydrate-based magnetic nanocomposites for effective cancer treatment. Int. J. Biol. Macromol. 1 (175), 281–293.
Sia, D., Villanueva, A., Friedman, S.L., Llovet, J.M., 2017. Liver cancer cell of origin, molecular class, and effects on patient prognosis. Gastroenterology 152, 745–761.
Skalickova, S., Milosavljevic, V., Cihalova, K., Horky, P., Richtera, L., Adam, V., 2017. Selenium nanoparticles as a nutritional supplement. Nutrition 33, 83–90.
Sklavos, A., Poutahidis, T., Giakoustidis, A., Makedou, K., Angelopoulou, K., Hardes, A., Andreani, P., Zacharioudaki, A., Saridis, G., Goulopoulos, T., Tsarea, K., Karamperi, M., Papadopoulos, V., Papanikolaou, V., Papalois, A., Iliadis, S., Mudan, S., Azoulay, D., Giakoustidis, D., 2018. Effects of wnt-1 blockade in DEN-induced hepatocellular adenomas of mice. Oncol. Lett. 15, 1211–1219.
Subedi, L., Venkatesan, R., Kim, S.Y., 2017. Neuroprotective and anti-inflammatory activities of allyl isothiocyanate through attenuation of JNK/NF-κB/TNF-signaling. Int. J. Mol. Sci. 18, 1423.
Sun, J., Kormakov, S., Liu, Y., Huang, Y., Wu, D., Yang, Z., 2018. Recent progress in metal-based nanoparticles mediated photodynamic therapy. Molecules 23 (2), 1704.
Tan, J.M., Karthivashan, G., Arulselvan, P., Fakurazi, S., Hussein, M.Z., 2014. Characterization and in vitro studies of the anticancer effect of oxidized carbon nanotubes functionalized with betulinic acid. Drug Des. Developm. Ther. 8, 2333–2343.
Tan, H., Mo, H.Y., Lau, A., Xu, Y.M., 2018. Selenium species: current status and potentials in cancer prevention and therapy. Int. J. Mol. Sci. 20 (1), 75.
Thomas, D.S., Fourkala, E.O., Apostolidou, S., GunuR, R.A., Jacobs, I., Menon, U., Alderton, W., Genty-Maharaj, A., Timms, J.F., 2015. Evaluation of serum CEA, CYFRA21-1 and CA125 for the early detection of colorectal cancer using longitudinal preclinical samples. Br. J. Cancer 113 (2), 268–274.
Tiernan, J.P., Perry, S.L., Verghese, E.T., West, N.P., Yeluri, S., Jayne, D.G., Hughes, T.A., 2013. Carcinoembryonic antigen is the preferred biomarker for in vivo colorectal cancer targeting. Br. J. Cancer 108 (3), 662–667.
Tripathi, K., Hussein, U.K., Anupalli, R., Barnett, R., Bachaboina, L., Scalici, J., Rocconi, R.P., Owen, L.B., Piazza, G.A., Palle, K., 2015. Allyl isothiocyanate induces replication-associated DNA damage response in NSCLC cells and sensitizes to ionizing radiation. Oncotarget 6, 5237–5252.
van der Meel, R., Sulheim, E., Shi, Y., Kiessling, F., Mulder, W.J.M., Lammers, T., 2019. Smart cancer nanomedicine. Nat. Nanotechnol. 14, 1007–1017.
Wagner, V., Dullaart, A., Bock, A.K., Zweck, A., 2006. The emerging nanomedicine landscape. Nat. Biotechnol. 24, 1211–1217.
Wang, Z., Li, Z., Ye, Y., Xie, L., Li, W., 2016. Oxidative stress and liver cancer: etiology and therapeutic targets. Oxid. Med. Cell Longev. 2016, 7891574.
Wang, Y., Tang, C., Zhang, H., 2015. Hepatoprotective effects of kaempferol 3-O-rutinoside and kaempferol 3-O-glucoside from Carthamus tinctorius L. on CCl4 induced oxidative liver injury in mice. J. Food Drug Anal. 23, 310.
Wathoni, N., Rusdin, A., Rebriani, E., Purnama, D., Daulay, W., Azhary, S.Y., Panatarani, C., Joni, I.M., Lesmana, R., Motoyama, K., Muchtaridi, M., 2019. Formulation and characterization of α-mangostin in chitosan nanoparticles coated by sodium alginate, sodium silicate, and polyethylene glycol. J. Pharm. Bioallied Sci. 11 (4), S619–S627.
Wen, C., Chao, H., Wu, L., Xu, L., Jiang, W., 2016. Rosmarinic acid inhibits inflammation and angiogenesis of hepatocellular carcinoma by suppression of NF-κB signaling in H22 tumor-bearing mice. J. Pharmacol. Sci. 132 (2), 131–137.
Wong, R.S., 2011. Apoptosis in cancer: from pathogenesis to treatment. J. Exp. Clin. Cancer Res. 30, 1–14.
Wu, C., Chen, Z., Hu, Y., Rao, Z., Wu, W., Yang, Z., 2018. Nanocrystals: the preparation, precise control and application toward the pharmaceutics and food industry. Curr. Pharm. Des. 24 (3), 2425–2431.
Wu, Z., Ma, X., Ma, Y., Yang, Z., Yuan, Y., Liu, C., 2020. Core/Shell PEGS/HA hybrid nanoparticle via micelle-coordinated mineralization for tumor-specific therapy. ACS Appl. Mater. Interfaces 12 (10), 12109–12119.
Xu, C., Shen, G., Yuan, X., Kim, J.H., Gopalkrishnan, A., Keum, Y.S., Nair, S., Kong, A.N., 2006. ERK and JNK signaling pathways are involved in the regulation of activator protein 1 and cell death elicited by three isothiocyanates in human prostate cancer PC-3 cells. Carcinogenesis 27, 437–445.
Yang, Z., Shi, J., Xie, J., et al., 2020. Large-scale generation of functional mRNA-encapsulating exosomes via cellular nanoporation. Nat. Biomed. Eng. 4 (2), 69–83.
Zhang, Z., Bi, M., Liu, Q., Yang, J., Xu, S., 2016. Meta-analysis of the correlation between selenium and incidence of hepatocellular carcinoma. Oncotarget 7 (47), 77110–77116.
Zhang, N., Yu, R., Cheng, X.Y., et al., 2018. Visual targeted therapy of hepatic cancer using homing peptide modified calcium phosphate nanoparticles loading doxorubicin guided by T1 weighted MRI. Nanomedicine.